Experimental Investigation of Al_2O_3 Nanofluid for Thermal Energy Management of Microchannel Heat Sink

Kapil R. Aglawe,[1*] **Ravindra K. Yadav,**[1] **and Sanjeev B. Thool** [2]

[1]Mechanical Engineering Department, National Institute of Technology, Raipur 492010, India.
[2]Mechanical Engineering Department, D. J. Sanghvi College of Engineering, Mumbai 400056, India.
[*]Correspondence should be addressed to Kapil R. Aglawe; kapilaglawe07@gmail.com

Received 9 December, 2022; Revised 15 December, 2022; Accepted 28 December, 2022
Available online 28 December, 2022 at www.atlas-tjes.org, doi: 10.22545/2022/00218

Energy is one of the primary foundations supporting evolutionary changes. Because of small size and improved heat transfer properties, nanofluid-cooled microchannel heat sinks (MCHS) have become a popular choice for electronics and thermal applications. The influence of employing nanofluids for cooling a chip was investigated experimentally in this work to evaluate the heat transfer characteristics. The investigations were carried out to confirm the influence of nanofluid concentration and wall temperature upon the thermal-hydraulic properties of the microchannel heat sink. In the present study, Al2O3 water nanofluid was employed, with 0.1, 0.2, 0.3, 0.4, and 0.5% nanoparticle volume fractions, mass flow rate (MFL) 2, 5, and 8 m/s at various inlet tempreture. The resulting experimental findings were verified from other researchers' results, which showed an important correlation. The heat transfer efficacy of electronics cooling systems has been enhanced by the nanofluid technology and configuration of rectangular heat sink.

Keywords: Microchannel heat sink, alumina (Al_2O_3), nanofluids, thermal management, CFD, experimentation, heat transfer enhancement.

1 Introduction

Energy is one of the primary foundations supporting evolutionary changes [1]. The performance of mobile phones, tablets, computers, and other electronic devices improves dramatically every year as new technologies emerge and processing frequencies increase [2]. With the increasing emphasis on processing speed in the electronics sector, the problem of excessive heat production has been solved straightforwardly [3], [4]. If the heat produced by such parts isn't properly evacuated, their useful life will be cut short very quickly [5]. The existing technology for cooling has reached its limits; hence new solutions must be developed [6]. Nanofluids with improved thermal characteristics have been shown to be effective coolants in heat transfer applications [7], [8]. Many types of nanoparticles (NPs) can be employed in the production of

nanofluids [9], [10]. Measurable increases in the coefficient of heat conductivity are the hallmark of such a process [11]. When it comes to cooling electronics, a higher integration level can generate a higher heat flux. Since the microelectronic device's reliability is highly dependent on its working temperature, consistency can decrease by as much as 5% for every additional degree above a temperature of 70 to 80°C [12].

Consequently, increasing the thermal conductivity is crucial to finding a solution to the heat transfer and flow difficulties that arise at the microscale [13]. However, due to the need for constructing more advanced processors, these coolants have hit their limits due to their restricted thermal conductivity (for example, 0.65 W/mC) [14]. As a result, there is a requirement to implement a new coolant to accelerate the process of convective cooling that takes place inside the MCHS [15], [16].

While working at the Argonne National Laboratory in the United States on a programme supported by the Department of Energy, Choi and Eastman presented nanofluids ideas [17]. Colloidal dispersion systems, which nanofluids are, are made up of the base fluid (dispersion medium) and NPs (dispersed phase) [3]. The distributed NPs have a thermal conductivity that is greater than a basic liquid [18]. As a result, high thermal conductivity is found in produced nanofluids [19]. In addition, the contact and collision that occurs between NPs, as well as those that occur between NPs and the substrate solution, contribute to a rise in the effective thermal conductivity of nanofluids [20], [21]. The activity of NPs might cause wear difficulties that are caused by particles that are millimeters and micrometers in size [22]. Therefore, the use of nanofluids as novel refrigerants for the purpose of enhancing heat transfer has garnered a significant amount of interest from academics, which has resulted in numerous novel advancements in a field of heat transfer [20], [23].

Utilizing nanofluids to enhance thermal properties has gained traction as a research focus in recent years. Compared to pure fluids, the newly created family of ultrafine (1-100 nm) nanofluid coolants demonstrated encouraging behavior in laboratory trials [24]. Ellsworth et al. [25] examined the history and development of water cooling systems, which included hybrid cooling in early IBM units and later transitioned to passive water cooling. To supply the necessary cooling power while maintaining simple operation at the module level, water refrigeration has been implemented [4]. For calculating a heat transfer and pressure decreases for a parallel plate MCHS, the author Xu et al. [26] investigated analytical approaches. Flow conditions and fine-geometry optimization minimize the entropy production rate. Limitations of air conditioning estimation based on numerical model and heat sink effects. Raghuraman et al. [27] conducted a computational investigation of an improved liquid flow features and heat transfer characteristics of rectangular MCHS. The medium of operation was water. The author Ali et al. [28] investigated the MCHS's experimental pressure drop and heat transfer characteristics. A cooling effectiveness of a TiO_2 nanofluid diluted to 15% by weight in water was compared to that of distilled water at 150 W, 125 W, and 100 W. The findings demonstrated that heat flow was crucial to TiO2 nanofluid's thermal efficiency and that its usefulness could be maximized at a reduced thermal cost. Graphene (GNP) nanofluids in water were also used to examine the angular influence on a pine-fin heat sink channel (0.25–0.75 LPM). Azari et al. [12] studied the laminar convective coefficient of an Al2O3 / water nanofluid under the same surface conditions in an experimental and numerical circular tube setup.

Systemic effects on the geometry sink base temperature microprocessor with nanofluid were investigated by [29]. They used a cylinder-shaped block of copper to run a 325-W heat-generating microprocessor and compared its performance to that of generally accessible nanofluids and heat sinks. They looked at thermal sink geometry's potential, which is sufficient to bring down the higher temperatures produced by microprocessors to adequate and safe levels. Using numerical methods, Seyf et al. [30] examined usage of nanofluids in micro-pin-fin MCHS. The heat transfer behavior of Micro-Pin-Fin MCHS was considered by solving the Navier-Stokes equation and 3-dimensional steady energy equation using a finite volume approximation and the SIMPLE method. NPs impact on the performance of a microprocessor designed to cool a central processing unit was investigated by [31]. Experiments and numerical analysis were first performed on distilled water, and afterward on two concentrations of CuO-water (0.86 and 2.25 vol. %) used as nano-fluids.

A innovative battery module design using two-layer nanofluids superior phase change medium was investigated by [32]. In this plan, n stands for main containers, m represents the cells, and p stands

for secondary containers. In two configurations (771 and 711), each Li-ion cell was allowed to discharge under three distinct settings [33]. The improvement in heat transport inside projecting heat sources was investigated by Sultan et al. [34]. In addition, he found a formula that relates the Nu to the Richardson number. Alumina nanofluids were analyzed for their thermal conductivity and viscosity by Shah et al. [35]. Their research demonstrated that a- Al_2O_3 nanofluid has greater thermal stability than common cooling fluids. From the heat source chilled by forced nanofluid flow, Esmaeil et al. [36] conducted tests for mixed convection heat transfer. Paraffin wax, an aluminum chip, and nano-silicon carbide (SiC) tubes were employed to enhance the heater's performance by [37]. The experimental findings showed that the new air heater worked well in Bagdad's climate. For cooling, Siricharoenpanicha et al. [38] utilized a combination of Ag and Fe_3O_4 nanofluids. It was taken into account how the flow rate, shape, and MCHS design would affect thermal dissipation.

Elsayed et al. [39] investigated the influence that utilizing helical coils in conjunction with nanofluids had on the thermal performance and the pressure drops that occurred in a turbulent flow pattern. The behavior of a nanofluid combination of Al2O3 NPs and water has been investigated by [40]. This mixture is now being pumped into a closed system designed to cool chips and other electronic equipment. The findings of the turbulent flow indicated that the inclusion of NPs in the distilled fluid significantly enhanced the rate of heat transfer. Additionally, the Glycol Ethylene was utilized for a cooling procedure, with volumes ranging from 30 to 50 percent [41].

This research aims to investigate how microprocessors' cooling is affected by utilizing Al_2O_3 nanofluids, each of which has a different volume proportion of NPs. A heating chip with dimensions of 5 centimeters by 5 centimeters and a power output of 130 watts may be cooled using thermal management technology. The Al_2O_3 NPs were combined in water at varying concentrations of 0.1, 0.2, 0.3, 0.4, and 0.5% the total volume. The mass flow rate of the flowing fluid was varied as 2, 5, and 8 m/s at 25, 30 and 35°C inlet temperature. This work uses experimental data, verified using data from previous studies and the literature.

2 Experimental Setup

This section discusses details about the experimental setup, methodology adopted for conduction of experiments, and the information about the test section.

2.1 Experimental Setup

Figure 1 shows the block diagram of an experimental setup used in the current study. The various components used in the experimental setup are a Coolant tank, Syringe pump, Digital differential pressure transducer, Microchannel test section, Rectangular cartridge heaters, Thermostat, Data Acquisition system, Computer, Radiator, Digital temperature indicator, and Glass wool.

With the help of a thermostat, heat is sent to the bottom of the MCHS from a rectangular cartridge heater with a capacity of 300 W and a thickness of 1.5 mm. The heat flux from this heater can range from 40 kW/m2 to 84 kW/m2. This experiment uses Al_2O_3 nanofluid with a volume concentration of 0.1% to 0.5%. The leakiness of the MCHS was first examined, and the sensors' ability to detect changes in temperature and pressure were validated while water was circulating through them. To keep the MFL stable, a regulator controlled the speed of the stepper motor. The fluid's MFL has been timed with a stopwatch. By changing the flow metre, we can keep the nanofluid flow rate constant at 0.1 LPM. The data for temperature and pressure were obtained during conditions of relative calm. The following standard correlation was used to compute the output.

Fei Yu et al. provide the heat transfer correlation [42] as in equation (1).

$$Q = mc(T_{out} - T_{in}) \tag{1}$$

Where, m – Mass flow rate; c - specific heat capacity.

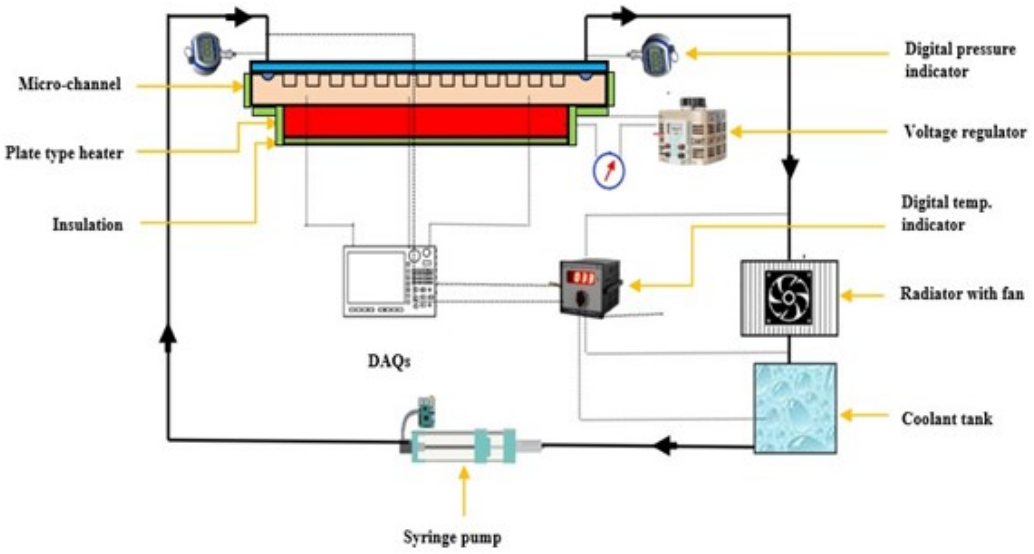

Figure 1: *Experimental setup block diagram.*

Ganapathy et al. provided the following equation for determining the typical Nusselt number [43] as in equation (2).

$$N_u = h_{exp}\frac{D_h}{k} \tag{2}$$

Where, k - thermal conductivity; D_h - hydraulic diameter of MCHS.

It is possible to get the heat transfer coefficient (HTC) by using equation (3) [44]

$$h = Q/((T_w - T_m) \times A_s \times 58) \tag{3}$$

Where, Q - heat carried by coolant, T_w, and T_m is the surface temperature of MCHS and mean temperature of the coolant, and as is the surface area of the channel. The equation (4) was used to figure out how much energy was needed for pumping.

$$P_P = \Delta_P \times V_c \times 58 \times 1000 \tag{4}$$

Where, V_c is the volume rate of flow. Yan Fan et al used to figure out the friction factor [45] by equation (5).

$$F_{exp} = 2 \times \delta_P/(L \times \rho \times U_c^2) \tag{5}$$

Where, U_c is a fluid velocity and L is MCHS length.

Figure 2 shows the pictorial view of an experimental set-up used in the current study. The various components used in the experimental set-up are Coolant tank (1), Syringe pump (2), Digital differential pressure transducer (3), Microchannel test section (4), Rectangular cartridge heaters (5), Thermostat (6), Data Acquisition system (7), Computer (8), Radiator (9), Digital temperature indicator (10) and Glass wool.

Table 1 displays the descriptions of specific parts employed in the experimental setup. The nanofluid was moved from the acrylic Coolant tank to the MCHS test section with the help of a syringe pump. The regulator on the stepper motor that ran the syringe pump was utilized to control a flow rate of a

Figure 2: *Typical experimental setup where Coolant tank (1), Syringe pump (2), Digital differential pressure transducer (3), Microchannel test section (4), Rectangular cartridge heaters (5), Thermostat (6), Data Acquisition system (7), Computer (8), Radiator (9), Digital temperature indicator (10) and Glass wool.*

Table 1: Specification of the experimental components

Components	Details
Microchannels	50 x 50 x 3 mm (L x W x H) d_h=0.2mm No of channel=58 Material: Copper
Syringe Pump	volume 22 ml (1 to 10 ml/sec)
Digital pressure indicator (Precision Engg. Pvt. Ltd.)	Pressure gauge range 0 to 100 Kpa
Rectangular cartridge heaters (Nichrome)	Max. Capacity 300 W 35*35mm
Dimmerstat	0 - 300 W
Thermocouple	k type 0ºC - 300 ºC ±0.1 ºC
Digital temperature indicator	-25 ºC – 250 ºC
Heat exchanger/Radiator (For closed system) Cross flow	Dimensions:(80*80*26)mm Material: Aluminum No. of Tube:08 Tube Diameter:1mm
Fluid tank	Acrylic 0.5 litre capacity
Data acquisition system	VKV Engineering Solution Pvt. Ltd.
Insulation	Glass Wool max capacity 1200 ºC

nanofluid. Nanofluid has a MFL that ranges from 0.1 lpm to 0.5 lpm. After the radiator and coolant tank, the temperature of the nanofluid flowing through the MCHS was measured using an Ambetronics K-type thermocouple with a measuring range of 0°C to 3000°C. A digital differential pressure transducer made by Setra that can measures pressure values from 0 to 100Kpa was attached to the outlet and inlet sides of a MCHS for measuring the difference in pressure.

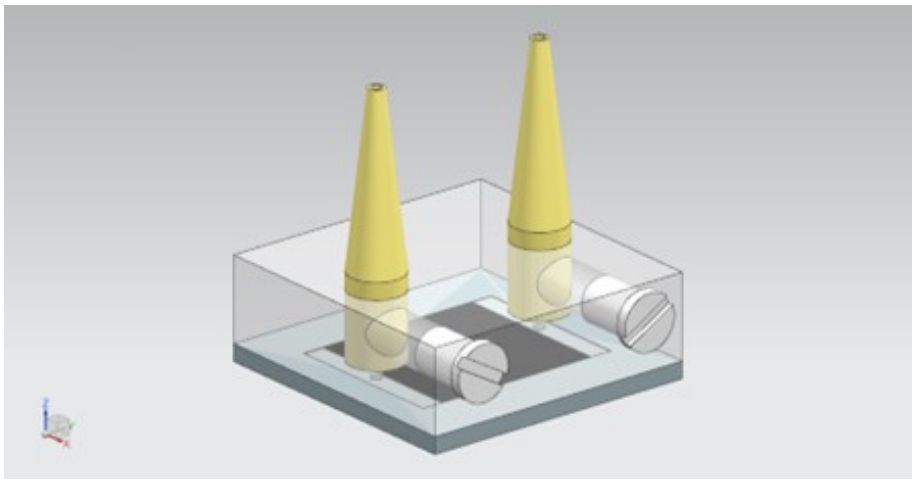

Figure 3: *CAD model microchannel assembly.*

At the bottom of the MCHS, three more thermocouples were added to measure a temperature of the bottom surface of the MCHS. The first is a copper plate heat sink with parallel MCHS. The second part is a piece of acrylic glass that is put over the MCHS so that the flow can be seen. The last part is a 2 mm-diameter nozzle that is placed above the acrylic glass so that nanofluid can flow through. The nanofluid can flow through the MCHS plate, which has channels for it to do so. The thermostat ensures that the rectangular cartridge heater at the bottom of the MCHS always gets the same heat. The nanofluid is cooled by a cross-flow type radiator that is attached to a MCHS test section and the reservoir. The data acquisition system sends the temperature of the MCHS to the computer.

2.2 Test Section Fabrication

CAD software was used to draw a model of a MCHS test section, and the vertical milling machine was used to do the machining. The MCHS was first cut to 50 mm x 50 mm and 3 mm thick for the straight parallel channels with a vertical milling machine. Then, a wire-cut EDM was used to cut channels in a copper plate to make the channels that were needed. MCHS was made in size of 35*35* mm with a hydraulic diameter of channel is 0.2 mm. The total number of channels is 58 and spacing between the channel is 0.5mm. Figure 3 shows CAD model of MCHS assembly.

At the top of the MCHS, a screw holds the acrylic glass that was cut with a CNC machine in place to stop leaks and let nanofluids flow through.

3 Results and Discussion

For cooling a MCHS, the current work experimentally examined the advantages of using an Al_2O_3-Water nanofluid over plain water. The heat transfer properties of Al_2O_3-Water nanofluid combinations are evaluated in a rectangular-shaped MCHS under varying circumstances.

3.1 Influence of Mass Flow Rate of Water at Heat Transfer Coefficient

Figure 4 shows the MFL effect of water at HTC with inlet temperature as 25°C, 30°C, and 35°C. By varying the MFL from 2 m/s to 8 m/s, the HTC are varied from 2847.38 to 8754.14, 2949.71 to 9550.42 and 3120.09 to 10066.73 W/m2K at 25°C, 30°C, and 35°C inlet temperature respectively. Highest HTC of

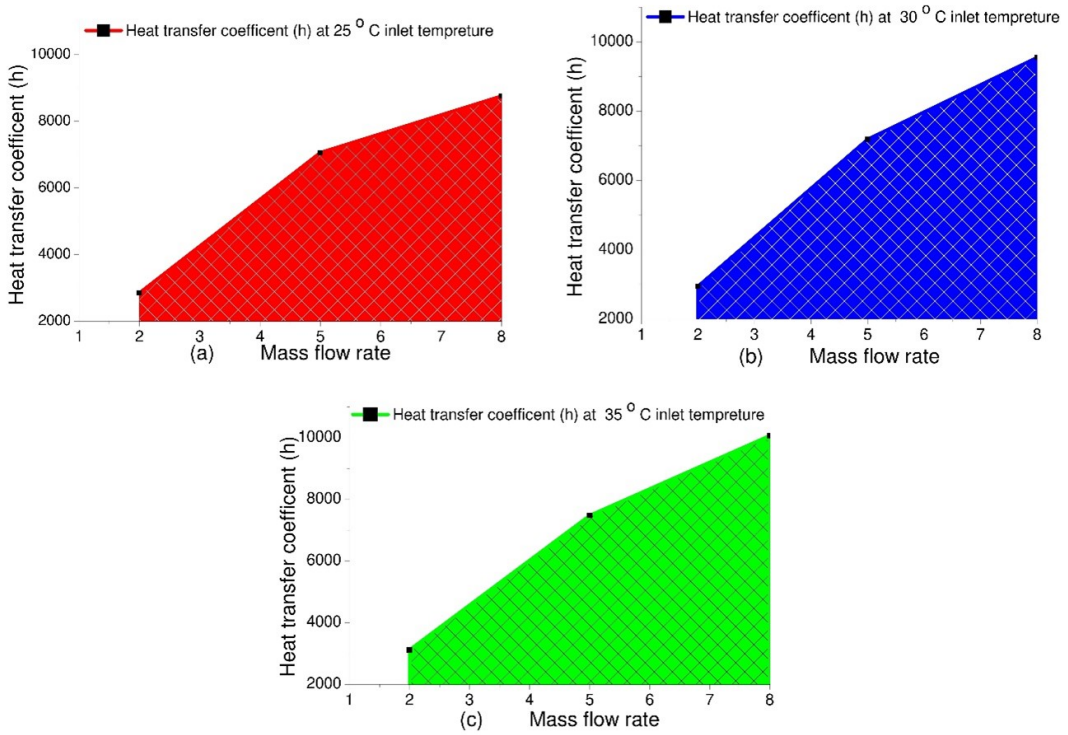

Figure 4: *Mass flow rate effect of water at heat transfer coefficient with varying inlet temperature.*

10066.73 W/m2k was observed at a MFL of 8 m/s at 35°C inlet temperature, whereas the lowest HTC of 2847.38 W/m^{2}K was observed at a MFL of 2 m/s at 25°C inlet temperature.

Compared to Al_2O_3 nanofluid, water is not very good at transferring heat. Because the water MFL has increased, the Reynolds number increased which made the HTC go up. The results of the experiment were very similar to those of the studies done by the [46].

3.2 Combined Influence of Mass Flow Rate, Nanofluid Concentration, and Inlet Temperature on Heat Transfer Coefficient

3.2.1 Influence of Mass Flow Rate and Nanofluid Concentration at 25° Inlet Temperature

Figure 5 shows the effect of MFL and % nanofluid concentration of Al2O3 nanofluid on HTC with inlet temperature as 25°C. By varying the nanofluid concentration from 0.1 to 0.5%, the HTC s are increased from 3156.14 to 4436.08, 8096.94 to 10514.16 and 11604.42 to 15044.68 W/m^{2}K for 2 m/s, 5 m/s, and 8 m/s respectively, at 25°C at inlet temperature. Highest HTC of 15044.68 W/m^{2}k was observed at a MFL of 8 m/s at 0.5% nanofluid concentration, whereas the lowest HTC of 3156.14 W/m^{2}K was observed at a MFL of 2 m/s at 0.1% nanofluid concentration.

The MFL and % nanofluid concentration of Al_2O_3 nanofluid have a considerable effect on the enhancement of the HTC such that with an increase in MFL and % nanofluid concentration, HTC increases considerably. Similar trend was found in the previous research carried out by various researchers. These findings are in a good agreement with the results reported in [46]. The average HTC was observed to increase with both the MFL and the % nanofluid concentration.

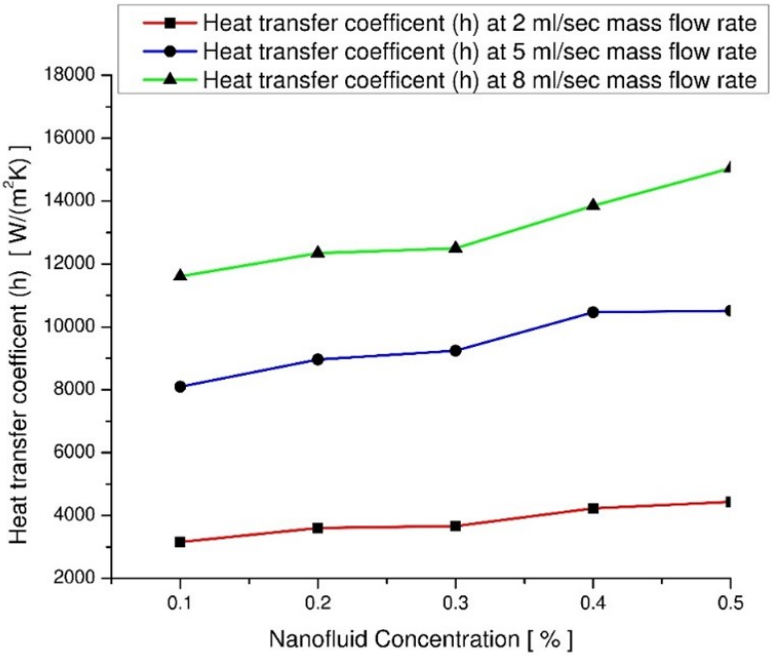

Figure 5: *Mass flow rate and nanofluid concentration at 25° inlet temperaturee.*

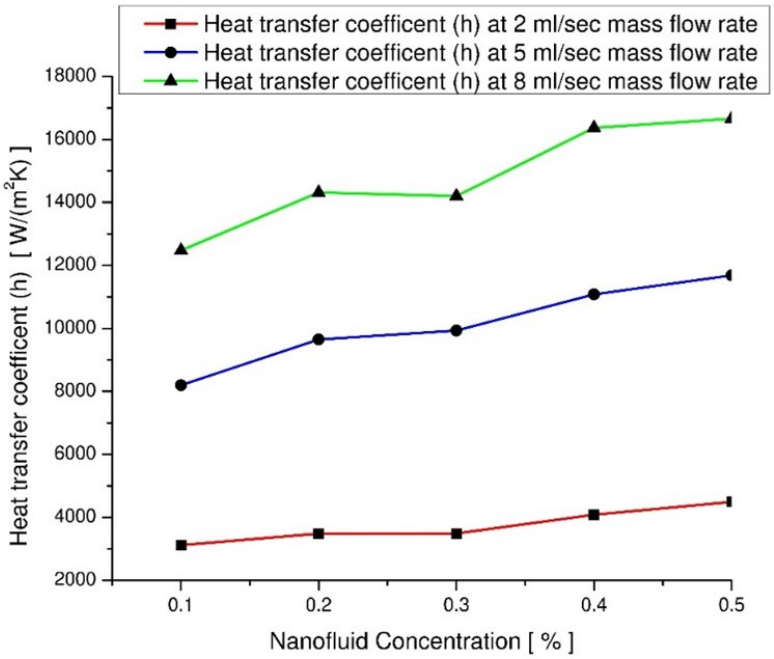

Figure 6: *Mass flow rate and nanofluid concentration at 30° inlet temperature.*

3.2.2 Influence of Mass Flow Rate and Nanofluid Concentration at 30° Inlet Temperature

Figure 6 shows the effect of MFL and % nanofluid concentration of Al_2O_3 nanofluid on HTC with inlet temperature as 30°C. By varying the nanofluid concentration from 0.1 to 0.5%, the HTC are increased

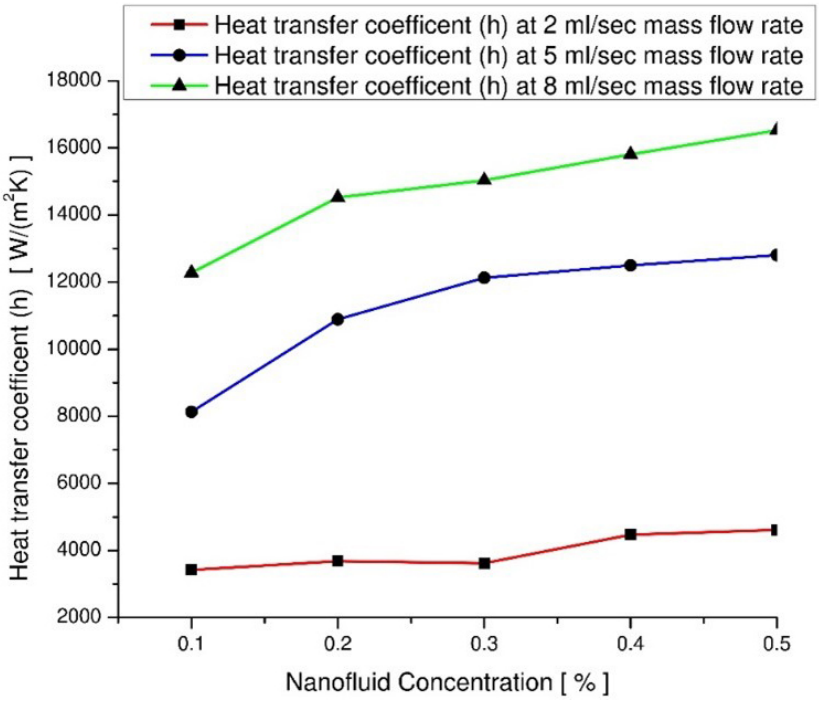

Figure 7: *Mass flow rate and nanofluid concentration at 35° inlet temperature.*

from 3119.22 to 4493.23, 8195.53 to 11684.54 and 12476.89 to 16656.84 W/m^{2}K for 2 m/s, 5 m/s, and 8 m/s respectively, at 30°C at inlet temperature. Highest HTC of 16656.84 W/m^{2}k was observed at a MFL of 8 m/s at 0.5% nanofluid concentration, whereas the lowest HTC of 3119.22 W/m^{2}K was observed at a MFL of 2 m/s at 0.1% nanofluid concentration.

The MFL and %nanofluid concentration of Al_2O_3 nanofluid have a significant influence on HTC enhancement, such that as MFL and % nanofluid concentration rise, HTC increases significantly. A similar pattern was discovered in prior study conducted by several academics. These findings are consistent with the findings published in [46]. Overall, the average HTC was shown to be intensified by MFL and % nanofluid concentration.

3.2.3 Influence of Mass Flow Rate and Nanofluid Concentration at 35° Inlet Temperature

Figure 7 shows the effect of MFL and %nanofluid concentration of Al_2O_3 nanofluid on HTC with inlet temperature as 35°C. By varying the nanofluid concentration from 0.1 to 0.5%, the HTC are increased from 3419.13 to 4615.24, 8131.95 to 12803.49 and 12280.97 to 16524.01 W/m^{2}K for 2 m/s, 5 m/s, and 8 m/s respectively, at 35°C at inlet temperature. Highest HTC of 16524.01 W/m^{2}k was observed at a MFL of 8 m/s at 0.5% nanofluid concentration, whereas the lowest HTC of 3419.13 W/m^{2}K was observed at a MFL of 2 m/s at 0.1% nanofluid concentration.

Both the MFL and the % nanofluid concentration of Al_2O_3 nanofluid play a key role in the enhancement of HTC, with the latter increasing dramatically when both parameters are raised. Several scholars have found a similar pattern in their own research. The results here agree with those found in [46]. On the whole, it was found that increasing the MFL and the concentration of nanofluids by a percentage both increased the HTC.

Experiments were conducted to determine an HTC of water and Al_2O_3-water nanofluids, and the findings are depicted in Figures 3 to 7. In this case, increasing the MFL results in a large rise in convective HTC of both Al_2O_3-water nanofluid and deionized water; nevertheless, the growth rate is very low. The

increase in the NPs mass fraction results in a rise in the average convective HTC of Al_2O_3-water nanofluids. The average convective HTC is significantly greater than or remains very close to the average convective HTC of 0.4% when the mass fraction of NPs is 0.5%. Both of these outcomes are favorable. The primary reason for this is that the thermal conductivity of NPs is noticeably higher than that of deionized water, and that the effective thermal conductivity is improved by any increase in the concentration of NPs. In other words, increasing the concentration of NPs improves effective thermal conductivity. NPs have the capacity to simultaneously increase the amount of disturbance in the fluid, reduce the amount of laminar substrate thickness, and lower the barrier to convection heat transfer.

However, as the concentration of NPs is increased, a further increase in the viscosity coefficient causes a slowing of movement and particle dispersion, which eventually results in a slower rate of heat transfer. It was also found that there was a significant connection between the temperature of the fluid when it was introduced into the system and the phenomena of the HTC. The HTC had a significant increase as a direct result of the increase in the temperature of the input, which went from 25 degrees Celsius to 35 degrees Celsius. The average convection HTC of Al_2O_3-water nanofluids is much higher than that of water as a flowing medium. This difference is significant enough to be statistically significant. This is mostly owing to the fact that Al_2O_3 has a higher density than water, and that molecules with a high density, small size, and that are packed tightly together will always improve heat transmission.

4 Conclusion

The thermal performance of an Al2O3-water nanofluid was tested inside a heat sink with a rectangular MCHS. From the results, following conclusions can draw:

1. The heat transfer characteristic was found to be enhanced at increasing concentrations of nanoparticles compared to lower percentages and pure water.
2. At a mass flow rate of 8 m/s and a concentration of 0.5% nanofluid, the maximum HTC is about 16524.01 W/m^2k.
3. Al_2O_3-water nanofluids demonstrated superior thermal performance compared to water as a flowing medium.
4. This study shows how the design of a rectangular MCHS geometry and the existence of a nanofluid mechanism can improve the thermal performance of electronic cooling.

Overall, the Al_2O_3-water nanofluids demonstrate plausible heat transfer capability, making them a suitable coolant for application in a MCHS. The friction factor and pressure drop need additional research before it can be used in a MCHS. Additional research is required to determine whether or not the presence of Al_2O_3-water nanofluids in the base fluid results in an increase in pressure drop.

Funding: This research received no external funding.

Conflicts of Interest: The authors declare no conflict of interest.

Authors Contributions: Co-authors contributed equally.

References

[1] Karpat, F., Kalay, O. C., Dirik, A. E., & Karpat, E. (2022). Fault Classification of Wind Turbine Gearbox Bearings Based on Convolutional Neural Networks. *Transdisciplinary Journal of Engineering and Science,* 13, 71–83. https://doi.org/10.22545/2022/00190

[2] Belkhode, P. N., Ganvir, V. N., Shelare, S. D., Shende, A., & Maheshwary, P. (2022). Experimental investigation on treated transformer oil (TTO) and its diesel blends in the diesel engine. *Energy Harvesting and Systems,* 9(1), 75–81. https://doi.org/10.1515/ehs-2021-0032

[3] Yavaş, Ö., Savran, E., Nalbur, B. E., & Karpat, F. (2022). Energy and Carbon Loss Management in an Electric Bus Factory for Energy Sustainability. *Transdisciplinary Journal of Engineering and Science,* 13, 97– 110. https://doi.org/10.22545/2022/00207

[4] Model, C. E. (2022). Exploring Grassroots Renewable Energy Transitions: Developing a. *Transdisciplinary Journal of Engineering & Science,*2, 137–163. https://doi.org/10.22545/2022/00215

[5] Shelare, S. D., Aglawe, K. R., & Belkhode, P. N. (2022). A review on twisted tape inserts for enhancing the heat transfer. *Materials Today: Proceedings,* 54, 560–565. https://doi.org/10.1016/j.matpr.2021.09.012

[6] Palande, D. D., Ghuge, N. C., & Dapase, C. R. (2022). Waste Heat Recovery From The Hot Water Boiling Plant Analysis using CFD. *Transdisciplinary Journal of Engineering and Science,* 13, 43–56. https://doi.org/10.22545/2022/00182

[7] Aglawe, K. R., Yadav, R. K., & Thool, S. B. (2021). Preparation, applications and challenges of nanofluids in electronic cooling: A systematic review.*Materials Today: Proceedings,* 43, 366–372. https://doi.org/10.1016/j.matpr.2020.11.679

[8] Gajbhiye, T., Shelare, S., & Aglawe, K. (2022). Current and Future Challenges of Nanomaterials in Solar Energy Desalination Systems in Last Decade. *Transdisciplinary Journal of Engineering & Science,* 13, 187–201. https://doi.org/10.22545/2022/00217

[9] Aglawe, K. R., Yadav, R. K., & Thool, S. B. (2022). Current Technologies on Electronics Cooling and Scope for Further Improvement: A Typical Review. *Proceedings of the International Conference on Industrial and Manufacturing Systems* (CIMS-2020), 389–408. https://doi.org/10.1007/978-3-030-73495-4_27

[10] Shelare, S. D., Aglawe, K. R., & Khope, P. B. (2021). Computer aided modeling and finite element analysis of 3-D printed drone. *Materials Today: Proceedings,* 47, 3375–3379. https://doi.org/10.1016/j.matpr.2021.07.162

[11] Kurnia, J. C., Haryoko, L. A. F., Taufiqurrahman, I., Chen, L., Jiang, L., & Sasmito, A. P. (2022). Optimization of an innovative hybrid thermal energy storage with phase change material (PCM) wall insulator utilizing the Taguchi method. *Journal of Energy Storage,* 49, 104067. https://doi.org/10.1016/j.est.2022.104067

[12] Azari, A., Kalbasi, M., & Rahimi, M. (2014). CFD and experimental investigation on the heat transfer characteristics of alumina nanofluids under the laminar flow regime. *Brazilian Journal of Chemical Engineering,* 31(2), 469–481. https://doi.org/10.1590/0104-6632.20140312s00001959

[13] Palande, D. D., Ghuge, N. C., & Shrivastwa, R. (2022). Comprehensive Review of Karanja & Jatropha Biodiesel Fuelled Diesel Engines. *Transdisciplinary Journal of Engineering and Science,* 13, 85–96. https://doi.org/10.22545/2022/00201

[14] Dhutekar, P., Mehta, G., Modak, J., Shelare, S., & Belkhode, P. (2021). Establishment of mathematical model for minimization of human energy in a plastic moulding operation.*Materials Today: Proceedings,* 47, 4502–4507. https://doi.org/10.1016/j.matpr.2021.05.330

[15] Bayomy, A. M., Saghir, M. Z., & Yousefi, T. (2016). Electronic cooling using water flow in aluminum metal foam heat sink: Experimental and numerical approach. *International Journal of Thermal Sciences,* 109, 182–200. https://doi.org/10.1016/j.ijthermalsci.2016.06.007

[16] Dhande, H. K., Shelare, S. D., & Khope, P. B. (2020). Developing a mixed solar drier for improved postharvest handling of food grains. *Agricultural Engineering International: CIGR Journal,* 22(4), 166–173.

[17] Eastman, J.A., Choi, U.S. (1997). Enhancing thermal conductivity through the development of nanofluids.*In Materials Research Society Symposium – Proceedings* (Vol. 457, pp. 3–11). https://www.osti.gov/servlets/purl/459378

[18] Waghmare, S., Shelare, S., Aglawe, K., & Khope, P. (2022). A mini review on fibre reinforced polymer composites. *Materials Today: Proceedings,* 54, 682–689. https://doi.org/10.1016/j.matpr.2021.10.379

[19] Xuan, Y., & Li, Q. (2000). Heat transfer enhancement of nanofluids. *International Journal of Heat and Fluid Flow,* 21(1), 58–64. https://doi.org/10.1016/S0142-727X(99)00067-3

[20] Belkhode, P. N., Shelare, S. D., Sakhale, C. N., Kumar, R., Shanmugan, S., Soudagar, M. E. M., & Mujtaba, M. A. (2021). Performance analysis of roof collector used in the solar updraft tower. *Sustainable Energy Technologies and Assessments,* 48, 101619. https://doi.org/10.1016/j.seta.2021.101619

[21] Belkhode, P. N., Ganvir, V. N., Shende, A. C., & Shelare, S. D. (2022). Utilization of waste transformer oil as a fuel in diesel engine. *Materials Today: Proceedings,* 49, 262–268. https://doi.org/10.1016/j.matpr.2021.02.008

[22] Hu, Z. S., & Dong, J. X. (1998). Study on antiwear and reducing friction additive of nanometer titanium oxide. *Wear,* 216(1), 92–96. https://doi.org/10.1016/S0043-1648(97)00252-4

[23] Sun, B., & Liu, H. (2017). Flow and heat transfer characteristics of nanofluids in a liquid-cooled CPU heat radiator. *Applied Thermal Engineering,* 115, 435–443. https://doi.org/10.1016/j.applthermaleng.2016.12.108

[24] Kamyar, A., Saidur, R., & Hasanuzzaman, M. (2012). Application of Computational Fluid Dynamics (CFD) for nanofluids. *International Journal of Heat and Mass Transfer,* 55(15), 4104–4115. https://doi.org/10.1016/j.ijheatmasstransfer.2012.03.052

[25] Ellsworth, M. J., Campbell, L. A., Simons, R. E., Iyengar, M. K., Schmidt, R. R., & Chu, R. C. (2008). The evolution of water cooling for IBM large server systems: Back to the future. *2008 11th IEEE Intersociety Conference on Thermal and Thermomechanical Phenomena in Electronic Systems,* I-THERM, 266–274. https://doi.org/10.1109/ITHERM.2008.4544279

[26] Xu, G., Guenin, B., & Vogel, M. (2004). Extension of air cooling for high power processors. Thermomechanical Phenomena in Electronic Systems -*Proceedings of the Intersociety Conference,* 1(858), 186–193. https://doi.org/10.1109/itherm.2004.1319172

[27] Raghuraman, D. R. S., Thundil Karuppa Raj, R., Nagarajan, P. K., & Rao, B. V. A. (2017). Influence of aspect ratio on the thermal performance of rectangular shaped micro channel heat sink using CFD code. *Alexandria Engineering Journal,* 56(1), 43–54. https://doi.org/10.1016/j.aej.2016.08.033

[28] Ali, H. M., & Arshad, W. (2017). Effect of channel angle of pin-fin heat sink on heat transfer performance using water based graphene nanoplatelets nanofluids. *International Journal of Heat and Mass Transfer,* 106, 465–472. https://doi.org/10.1016/j.ijheatmasstransfer.2016.08.061

[29] Jajja, S. A., Ali, W., Ali, H. M., & Ali, A. M. (2014). Water cooled minichannel heat sinks for microprocessor cooling: Effect of fin spacing. *Applied Thermal Engineering,* 64(1), 76–82. https://doi.org/10.1016/j.applthermaleng.2013.12.007

[30] Seyf, H. R., & Feizbakhshi, M. (2012). Computational analysis of nanofluid effects on convective heat transfer enhancement of micro-pin-fin heat sinks.*International Journal of Thermal Sciences,* 58, 168–179. https://doi.org/10.1016/j.ijthermalsci.2012.02.018

[31] Al-Rashed, M. H., Dzido, G., Korpyś, M., Smołka, J., & Wójcik, J. (2016). Investigation on the CPU nanofluid cooling. *Microelectronics Reliability,* 63, 159–165. https://doi.org/10.1016/j.microrel.2016.06.016

[32] Jilte, R., Afzal, A., & Panchal, S. (2021). A novel battery thermal management system using nano-enhanced phase change materials. *Energy,* 219, 119564. https://doi.org/10.1016/j.energy.2020.119564

[33] Sahu, P., Shelare, S., & Sakhale, C. (2020). Smart cities waste management and disposal system by smart system: A review. *International Journal of Scientific and Technology Research,* 9(3), 4467–4470.

[34] Sultan, G. I. (2000). Enhancing forced convection heat transfer from multiple protruding heat sources simulating electronic components in a horizontal channel by passive cooling. *Microelectronics Journal,* 31(9), 773–779. https://doi.org/10.1016/S0026-2692(00)00058-6

[35] Shah, J., Ranjan, M., Davariya, V., Gupta, S. K., & Sonvane, Y. (2017). Temperature-dependent thermal conductivity and viscosity of synthesized α-alumina nanofluids. *Applied Nanoscience,* 7(8), 803–813. https://doi.org/10.1007/s13204-017-0594-7

[36] Esmaeil, K. K., Sultan, G. I., Al-Mufadi, F. A., & Almasri, R. A. (2019). Experimental Heat Transfer From Heating Source Subjected to Rigorous Natural Convection Inside Enclosure and Cooled by Forced Nanofluid Flow. *Journal of Heat Transfer,* 141(7). https://doi.org/10.1115/1.4043673

[37] Jawad, Q. A., Mahdy, A. M. J., Khuder, A. H., & Chaichan, M. T. (2020). Improve the performance of a solar air heater by adding aluminum chip, paraffin wax, and nano-SiC. Case Studies in Thermal Engineering, 19, 100622. https://doi.org/10.1016/j.csite.2020.100622

[38] Siricharoenpanich, A., Wiriyasart, S., Srichat, A., & Naphon, P. (2020). Thermal cooling system with Ag/Fe3O4 nanofluids mixture as coolant for electronic devices cooling. Case Studies in Thermal Engineering, 20, 100641. https://doi.org/10.1016/j.csite.2020.100641

[39] Elsayed, A., Al-dadah, R. K., Mahmoud, S., & Rezk, A. (2015). Numerical investigation of turbulent flow heat transfer and pressure drop of Al_2O_3/water nanofluid in helically coiled tubes. *International Journal of Low-Carbon Technologies,* 10(3), 275–282. https://doi.org/10.1093/ijlct/ctu003

[40] Nguyen, C. T., Desgranges, F., Roy, G., Galanis, N., Maré, T., Boucher, S., & Angue Mintsa, H. (2007). Temperature and particle-size dependent viscosity data for water-based nanofluids – Hysteresis phenomenon. *International Journal of Heat and Fluid Flow,* 28(6), 1492–1506. https://doi.org/10.1016/j.ijheatfluidflow.2007.02.004

[41] Waghmare, S. N., Shelare, S. D., Tembhurkar, C. K., & Jawalekar, S. B. (2020). Pyrolysis system for environment-friendly conversion of plastic waste into fuel. In Lecture Notes in Mechanical Engineering (pp. 131–138). Springer. https://doi.org/10.1007/978-981-15-4748-5_13

[42] Yu, X., Zhang, C., Teng, J., Huang, S., Jin, S., Lian, Y., Cheng, C., Xu, T., Chu, J.-C., Chang, Y.-J., Dang, T., & Greif, R. (2012). A study on the hydraulic and thermal characteristics in fractal tree-like microchannels by numerical and experimental methods. *International Journal of Heat and Mass Transfer,* 55(25), 7499–7507. https://doi.org/10.1016/j.ijheatmasstransfer.2012.07.050

[43] Ganapathy, H., Shooshtari, A., Choo, K., Dessiatoun, S., Alshehhi, M., & Ohadi, M. (2013). Volume of fluid-based numerical modeling of condensation heat transfer and fluid flow characteristics in microchannels. *International Journal of Heat and Mass Transfer,* 65, 62–72. https://doi.org/10.1016/j.ijheatmasstransfer.2013.05.044

[44] Shelare, S., Kumar, R., & Khope, P. (2021). Assessment of Physical, Frictional and Aerodynamic Properties of Charoli (buchanania Lanzan Spreng) Nut as Potentials for Development of Processing Machines. *Carpathian Journal of Food Science and Technology,* 13(2), 174–191. https://doi.org/10.34302/crpjfst/2021.13.2.16

[45] Fan, Y., Lee, P. S., Jin, L.-W., & Chua, B. W. (2013). A simulation and experimental study of fluid flow and heat transfer on cylindrical oblique-finned heat sink. *International Journal of Heat and Mass Transfer,* 61, 62–72. https://doi.org/10.1016/j.ijheatmasstransfer.2013.01.075

[46] Vinoth, R., & Sachuthananthan, B. (2021). Flow and heat transfer behavior of hybrid nanofluid through microchannel with two different channels. *International Communications in Heat and Mass Transfer,* 123, 105194. https://doi.org/10.1016/j.icheatmasstransfer.2021.105194

About the Authors

Kapil R. Aglawe is presently pursuing his Doctor of Philosophy (PhD) degree in the area of Mechanical Engineering, from the Mechanical Engineering, National Institute of Technology, Raipur, India. Also, he is working as an Assistant Professor in the Department of Mechanical Engineering at Priyadarshini College of Engineering, Nagpur, Maharashtra, India. He is pursuing his the Doctor of Philosophy (PhD) degree in the area of Mechanical Engineering, from the Mechanical Engineering, National Institute of Technology, Raipur, India. He has published more than 10 research articles throughout the several SCI / Scopus indexed journal, including International / National level conferences. He is also academically engaged with the reviewership with the several SCI/ Scopus indexed Journals from last 2 years. He is a life time member of several reputed professional societies at National and International level. Also he has a patent in his credentials in the field of Mechanical Engineering.

Dr. R. K. Yadav is presently working as an Associate Professor in the Department of Mechanical Engineering at National Institute of Technology, Raipur, India. He has received the Doctor of Philosophy (PhD) degree in the area of Mechanical Engineering, from Mechanical Engineering, National Institute of Technology, Raipur, India. He has published several number of research articles throughout SCI / Scopus indexed journal, including International / National level conferences. He is also academically engaged with the reviewership with the several SCI/ Scopus indexed Journals/ Conferences. He has delivered several Expert Talks/Lectures at different level of platform throughout the country. He is a life time member of several reputed professional societies at National and International level.

Dr. Sanjeev B. Thool is presently working as an Associate Professor in the Department of Mechanical Engineering at Dwarkadas Jivanlal Sanghvi College of Engineering, also known as D. J. Sanghvi, is an engineering college, Mumbai, Maharashtra, India. He has received the Doctor of Philosophy (PhD) degree in the area of Mechanical Engineering, from Mechanical Engineering, National Institute of Technology, Raipur, India. He has published several number of research articles throughout SCI / Scopus indexed journal, including International / National level conferences. He is also academically engaged with the reviewership with the several SCI/ Scopus indexed Journals/ Conferences. He has delivered several Expert Talks/Lectures at different level of platform throughout the country. He is a life time member of several reputed professional societies at National and International level. During his academic career he has authored two books of international publishers.